Free Radical Biology & Medicine, Vol. 29, No. 6, pp. 568–579, 2000

0891-5849/00/$–see front matter

PII S0891-5849(00)00407-X

Original Contribution

EPR DETECTION OF LIPID-DERIVED FREE RADICALS FROM PUFA, LDL, AND CELL OXIDATIONS

STEVEN YUE QIAN, HONG P. WANG, FREYA Q. SCHAFER, and GARRY R. BUETTNER
Free Radical Research Institute/ESR Facility, The University of Iowa, Iowa City, IA, USA

(*Received* 10 *August* 1999; *Revised* 5 *May* 2000; *Accepted* 1 *June* 2000)

Abstract—We have used the spin trap 5,5-dimethyl-pyrroline-1-oxide (DMPO) and EPR to detect lipid-derived radicals ($L_d^{\bullet}$) during peroxidation of polyunsaturated fatty acids (PUFA), low-density lipoprotein (LDL), and cells (K-562 and MCF-7). All oxygen-centered radical adducts of DMPO from our oxidizable targets have short lifetimes (<20 min). We hypothesized that the short lifetimes of these spin adducts are due in part to their reaction with radicals formed during lipid peroxidation. We proposed that stopping the lipid peroxidation processes by separating oxidation-mediator from oxidation-substrate with an appropriate extraction would stabilize the spin adducts. To test this hypothesis we used ethyl acetate to extract the lipid-derived radical adducts of DMPO (DMPO/$L_d^{\bullet}$) from an oxidizing docosahexaenioc acid (DHA) solution; Folch extraction was used for LDL and cell experiments. The lifetimes of DMPO spin adducts post-extraction are much longer (>10 h) than the spin adducts detected without extraction. In iron-mediated DHA oxidation we observed three DMPO adducts in the aqueous phase and two in the organic phase. The aqueous phase contains DMPO/$HO^{\bullet}$ ($a^N \approx a^H \approx 14.8$ G) and two carbon-centered radical adducts ($a^N{}_1 \approx 15.8$ G, $a^H{}_1 \approx 22.6$ G; $a^N{}_2 \approx 15.2$ G, $a^H{}_2 \approx 18.9$ G). The organic phase contains two long-chain lipid radical adducts ($a^N \approx 13.5$ G, $a^H \approx 10.2$ G; and $a^N \approx 12.8$ G; $a^H \approx 6.85$ G, 1.9 G). We conclude that extraction significantly increases the lifetimes of the spin adducts, allowing detection of a variety of lipid-derived radicals by EPR. © 2000 Elsevier Science Inc.

Keywords—EPR, Free radicals, Lipid peroxidation, Photosensitizer, Singlet oxygen, Spin trapping

INTRODUCTION

Determination of the radical species formed during lipid peroxidation is essential for the understanding of the free radical mechanisms by which cells are damaged and killed. In free radical-mediated lipid peroxidation many different kinds of lipid-derived radicals ($L_d^{\bullet}$, Scheme 1) can be produced [1–4]. They are carbon-centered radicals (lipid alkyl $L^{\bullet}$, β-scission alkyl $R^{\bullet}$, epoxyallylic $OL^{\bullet}$) and oxygen-centered radicals (alkoxyl $LO^{\bullet}/RO^{\bullet}$, peroxyl $LOO^{\bullet}/ROO^{\bullet}$, and epoxyperoxyl $OLOO^{\bullet}$). Using α-[4-pyridyl 1-oxide]-N-*tert*-butyl nitrone (POBN), we have been successful in the EPR spin trapping of carbon-centered radicals from intact cells during lipid peroxidation [5–8]. POBN adduct formation during cellular lipid peroxidation correlates well with cell membrane damage as measured by the TBAR assay and Trypan blue dye exclusion [9–11].

However, POBN is only an efficient spin trap for carbon-centered radicals derived from β-scission of lipid alkoxyl radicals (Scheme 1) during lipid peroxidation. It is believed that these carbon-centered radicals are less cytotoxic than the oxygen-centered radicals due to their lower reactivity and their location [1,2]. Thus, it is important to develop methods to detect oxygen-centered lipid radicals such as lipid alkoxyl ($LO^{\bullet}$) and lipid peroxyl radicals ($OLOO^{\bullet}$ or $LOO^{\bullet}$) in order to understand their detrimental roles in lipid peroxidation. Using EPR with DMPO spin trapping, Chamulitrat et al. and Davies et al. detected oxygen-centered lipid radicals in enzyme-dependent hydroperoxide reactions [12–14]; Schaich et al. detected these types of radicals with organic extraction from lipid solutions [15]. To our knowledge, there is no report on the successful EPR detection of oxygen-centered lipid radicals produced during membrane lipid peroxidation of intact cells.

The free radicals produced during lipid peroxidation

Address correspondence to: Garry R. Buettner, Free Radical Research Institute, EMRB 68, The University of Iowa, Iowa City, IA 52242-1101, USA; Tel: (319) 335-6749; Fax: (319) 335-8049; E-Mail: garry-buettner@uiowa.edu.

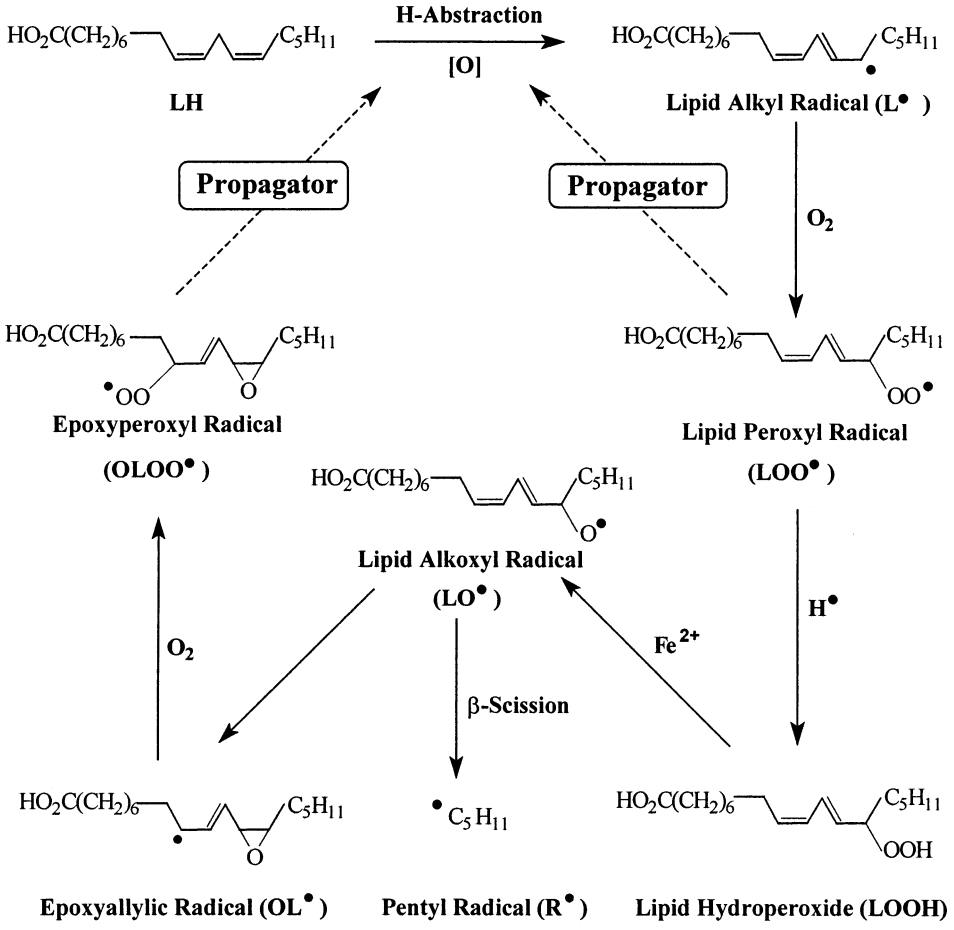

Scheme 1. An overview of the chemistry of the formation of lipid-derived radicals ($L_d^{\bullet}$) produced during lipid peroxidation in the presence of ferrous iron. This scheme shows some of the radical species formed in the peroxidation of linoleic acid. Three different propagating species are shown. It is currently thought that $OLOO^{\bullet}$ may be the major propagating species in this type of system [1,2]. The species $LO^{\bullet}$ is thought to be a very minor propagating species because of its very short lifetime. It is estimated that the rate constant of cyclization of $LO^{\bullet}$ would be $\sim 2 \times 10^7\ s^{-1}$ while the rate constant for β-scission would be $\sim 1 \times 10^6\ s^{-1}$ [40].

can undergo various termination reactions (reaction 2) that compete with the spin trapping reaction (reaction 1). However, these radicals can also react with the DMPO spin adducts that have been formed (reaction 3).

$$DMPO + {}^{\bullet}L_d \rightarrow DMPO/{}^{\bullet}L_d(\text{Spin Adduct}) \quad (1)$$

$${}^{\bullet}L_d + {}^{\bullet}L_d \rightarrow \text{Nonradical products} \quad (2)$$

$$DMPO/{}^{\bullet}L_d + {}^{\bullet}L_d \rightarrow \text{Nonradical product} \quad (3)$$

Peroxyl radicals react with nitroxides with rate constants of 10^4–$10^5\ M^{-1}s^{-1}$, while alkyl radicals, such as the carbon-centered radicals produced during lipid peroxidation, react at rates approaching the diffusion-controlled limit ($k \approx 10^{10}\ M^{-1}s^{-1}$) [16]. Thus, reaction 3 will be a significant route to the destruction of the spin adducts formed during lipid peroxidation. Therefore, we hypothesized that the destruction of DMPO spin adducts by these alkyl radicals (reaction 3) is a major reason the use of spin trapping for the detection of lipid radicals is so difficult. In the past, organic extraction has been used to advantage to isolate lipid-soluble spin adducts [14,17–19]. We propose that EPR spin trapping followed by extraction can overcome the problem of spin adduct destruction. The extraction process will separate iron ions (aqueous phase) from the oxidizable lipids (organic phase), thereby slowing or stopping the lipid peroxidation cycle (Scheme 2), and consequently slowing the reactions that destroy the spin adducts (reaction 3).

To test our hypothesis, we used ethyl acetate to extract the DMPO lipid radical adducts derived from DHA oxidation; we used Folch extraction ($CHCl_3/CH_3OH$) for LDL and cell oxidation experiments. The extraction method was used to separate the oxidizable substrates (lipids) from the mediator of oxidation (iron), Scheme 2. This separation interrupts the lipid peroxidation pro-

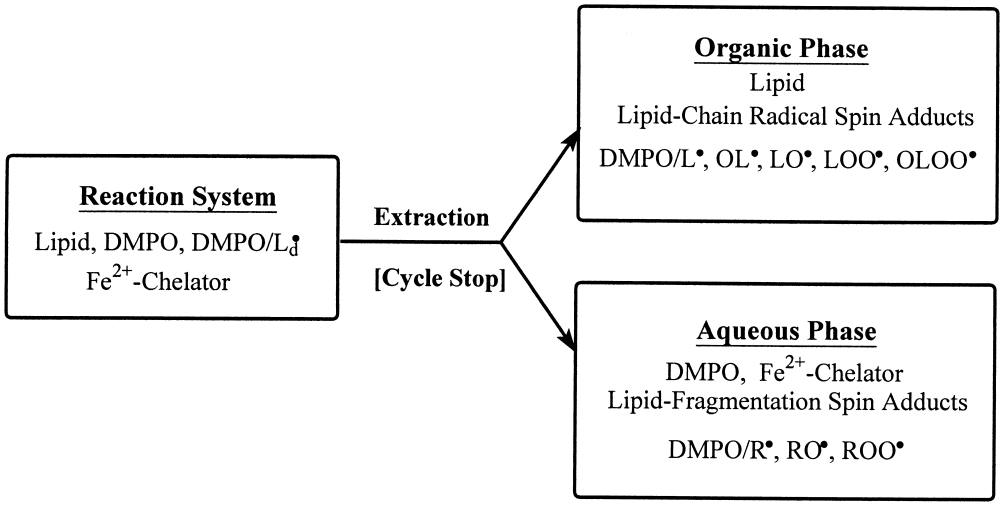

Scheme 2. Outline of how the different components of the lipid spin trapping system partition after extraction of the complete reaction system using an organic solvent, such as ethyl acetate or Folch extraction. Here, $L_d^{\bullet}$ represents all the potential lipid-derived radicals that could be spin trapped by DMPO; *L* represents the long-chain lipid species; and *R* represents the short-chain fragmentation products that can be produced during lipid peroxidation. In our experimental protocol, the organic phase of the extraction is evaporated to dryness using argon or nitrogen. Nitrogen-purged ethyl acetate is used to redissolve the spin adducts for EPR examination. Using this protocol any DMPO as well as small molecular weight spin adducts (volatile), such as DMPO/$HO^{\bullet}$, that have partitioned into the organic phase have been removed, leaving only the long-chain fatty acids and long-chain radical adducts. The removal of DMPO also avoids the formation of additional spin adducts in the organic phase after extraction. The aqueous phase is observed directly.

cesses thereby stabilizing the DMPO/$L_d^{\bullet}$ spin adducts by minimizing reaction 3, as well as by dilution of reactants and products. For all experimental models, the lifetimes of DMPO lipid-derived radical adducts post-extraction are much longer (>10 h) than the experimental lifetimes of DMPO radical adducts without extraction (<20 min). Furthermore, combining EPR spin trapping with an extraction process provides the opportunity to detect different types of radical adducts in different phases. Long-chain lipid radicals are detected dominantly in the organic phase, while the small fragment radicals ($R^{\bullet}$, $HO^{\bullet}$, $RO^{\bullet}$) are mostly present in the aqueous phase. We find that our extraction will allow us to distinguish radical adducts via their hydrophilic or hydrophobic nature, in addition to their hyperfine splitting constants. This will allow the identification of radicals that have similar hyperfine splittings, but quite different physical properties. This protocol offers new possibilities for studying these unstable species and the complex events of lipid peroxidation.

EXPERIMENTAL PROCEDURES

Chemical reagents

All DHA experiments were performed in 50 mM potassium phosphate-buffer (PB, pH 7.4). All cell experiments were performed in 50 mM potassium phosphate-buffer saline (PBS, pH 7.4). Adventitious metals in PB and PBS were removed by treatment with chelating resin (sodium form, dry mesh 50–100, from Sigma, St. Louis, MO, USA) using the batch method. The absence of metal was verified with the ascorbate test [20]. The spin trap DMPO, 5,5-dimethyl-pyrroline-1-oxide (Sigma) was first purified with activated charcoal/benzene, and then prepared as a 1.0 M aqueous stock solution [21]. During the experiment this DMPO stock solution was kept on ice. Ferrous ammonium sulfate ($Fe(NH_4)_2(SO_4)_2 \cdot 6H_2O$, Fisher Scientific Co. Fair Lawn, NJ, USA) and copper sulfate ($CuSO_4 \cdot 5H_2O$, Fisher Scientific Co.) were used to prepare 10 mM stock solutions of Fe^{2+} and Cu^{2+} in 0.01 N HCl. Diethylenetriaminepentaacetic acid (DTPA, Sigma) was prepared as a 10 mM neutral stock solution. Docosahexaenoic acid (DHA, Sigma) was prepared as a 5 mM aqueous stock solution immediately before the EPR spin trapping experiment. Photofrin stock solution (porfimer sodium, QLT, Phototherapeutics, Inc., Vancouver, BC, Canada) was dissolved in 5% dextrose (3 mg/ml, pH 7.4), sterile filtered and stored at −20°C.

LDL

Low-density lipoprotein was obtained from Dr. S. Hempel's Lab, University of Iowa. EDTA (1 mg/ml) was present throughout the isolation and dialysis to prevent LDL oxidation [22]. A typical incubation for EPR experiments consisted of 2.2 mg protein/ml of LDL, 100 mM DMPO, and 100 μM Cu^{2+} in PB. To analyze spin adducts in the PB-LDL suspension, the incubation mix-

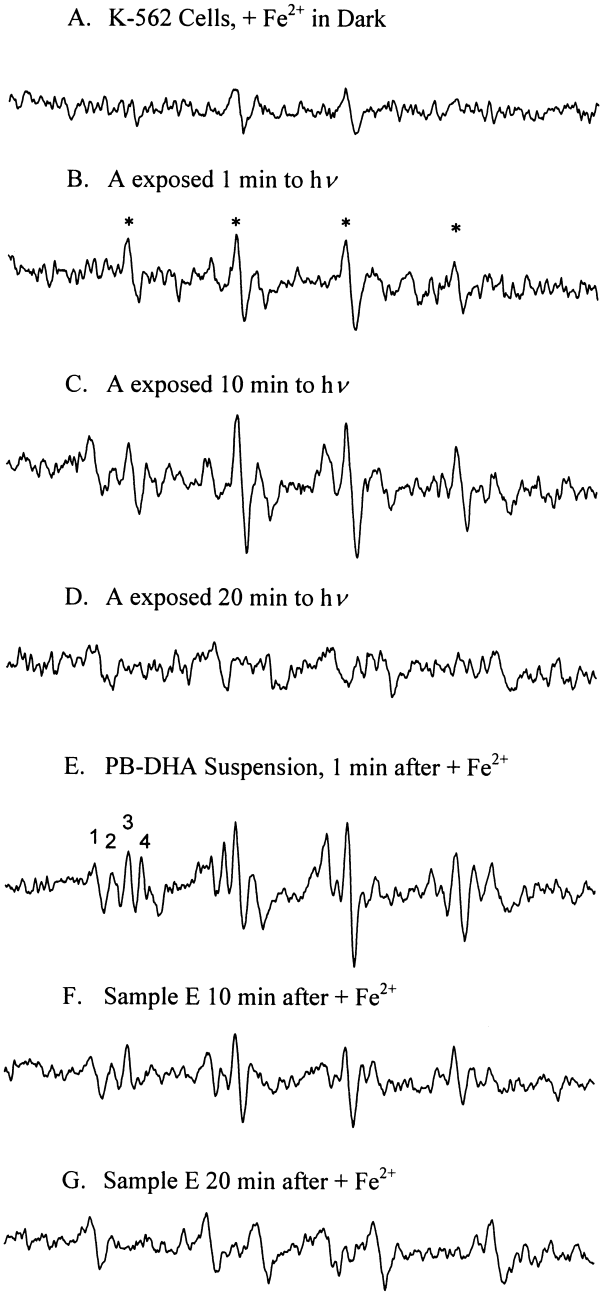

Fig. 1. EPR spectra of DMPO/$L_d^{\bullet}$ formed from Photofrin-mediated membrane lipid peroxidation in K-562 cells (A–D) and Fe^{2+}-mediated DHA oxidation (E–G). Spectra change with time, indicating an evolving balance between adduct formation and adduct decay. (A) EPR spectrum of DMPO/$L_d^{\bullet}$ from K-562 cells (2×10^7 cells/ml) pretreated with 9 μg/ml Photofrin (45 min) but not exposed to light. The K-562 cells were enriched with DHA; cell peroxidation was initiated by addition of 100 μM Fe^{2+} in the presence of 150 mM DMPO, 250 μM O_2, and 110 μM DTPA; (B) 1 min light exposure (180 W/m^2) of A. The hyperfine splittings of the major spin adduct marked by * are: $a^N \approx a^H \approx 14.8$ G; (C) 10 min light exposure (180 W/m^2) of A. The additional major spin adduct hyperfine splittings are: $a^N \approx 15.8$ G, $a^H \approx 22.6$ G; (D) 20 min light exposure (180 W/m^2) of A. Only one spin adduct with $a^N \approx 15.8$ G, $a^H \approx 22.6$ G was observed; (E) EPR spectrum from 5 mM DHA incubated with 250 μM O_2, 50 mM DMPO, 110 μM DTPA, and 100 μM Fe^{2+}. This EPR spectrum was collected beginning 1 min after Fe^{2+} addition. There are four different spin adducts: $a_1^N \approx 15.8$ G, $a_1^H \approx 22.6$ G; $a_2^N \approx 15.2$ G, $a_2^H \approx 18.9$ G, $a_3^N \approx a_3^H \approx 14.8$ G; $a_4^N \approx 14.6$ G, $a_4^{H\beta} \approx 10.2$ G; $a_4^{H\gamma} \approx 1.3$ G; (F) EPR spectrum from sample E, but spectrum collection was initiated 10 min after Fe^{2+} addition. This spectrum shows a loss of DMPO adducts compared to E; (G) EPR spectrum from sample E, but collection was initiated 20 min after Fe^{2+} addition. Only one radical adduct ($a_1^N \approx 15.8$ G, $a_1^H \approx 22.6$ G) can be detected at this time. All spectra are from 12 signal-averaged scans collected over a total of 2 min.

ture (500 μl) was transferred into an EPR flat cell for EPR measurement. For analysis of spin adducts, the incubation mixture (500 μl) was extracted by Folch extraction before EPR measurements.

Suspension cells

K-562 cells were grown in RPMI 1640 medium (Grand Island Biochemical Co., Grand Island, NY, USA) containing 10% fetal bovine serum (Sigma). Cell lipids were modified by supplementation of the medium with 32 μM DHA for 48 h [23–25]. Before the oxidation experiments, cells were washed three times with PBS (centrifuged at 300 $\times$ g for 5 min) and resuspended in 500 μl PBS with 150 mM DMPO at a density of 5×10^6 or 2×10^7cells/ml. After oxidative stress, such as Photofrin/light treatment, and addition of Fe^{2+}, PBS-suspended cells were transferred into an EPR flat cell for measurement of radical formation.

EPR measurement

The EPR samples (500 μl) were: 5 mM DHA in PB; 2.2 mg/ml LDL in PB; or K-562 cells suspended in PBS (5×10^6 or 2×10^7cells/ml). Two min after introduction of DMPO (50 mM for DHA experiments, 100 mM for LDL, or 150 mM for cell experiments) to the sample, oxidative stress was initiated and the sample was immediately transferred into a flat cell for EPR measurement. All EPR spectra were obtained with a Bruker ESP-300 spectrometer operating at 9.76 GHz and room temperature. The EPR spectrometer settings were modulation frequency 100 kHz; modulation amplitude 1.0 G; microwave power 40 mW, receiver gain 10^5–10^6. To assist in the assignment of spin adducts, comparisons were made with published values tabulated in the Spin Trapping Database at http://epr.niehs.nih.gov/stdb1.html [26], as well as other tabulations [27].

Ethyl acetate extraction

The 5 mM DHA samples (500 μl) were extracted with 5 ml ethyl acetate (saturated with ice-cold water). Samples were kept at room temperature until phase separa-

tion (30 min–2 h). The upper ethyl acetate phase was removed and evaporated with N_2 or Ar, and then resuspended in 500 μl nitrogen-saturated ethyl acetate for EPR measurement of lipid radicals.

Folch extraction for LDL and K-562 cells

LDL (2.2 mg/ml) or K-562 cells (5×10^6 cells/ml) in 500 μl PB or PBS were extracted with 3 ml ice-cold methanol:6 ml $CHCl_3$:1.5 ml 0.9% sodium chloride. Samples were kept at room temperature overnight to allow phase separation. The bottom phase ($CHCl_3$) was transferred into 15 ml tubes and purged with nitrogen. After complete evaporation, the lipid products were resuspended in 500 μl nitrogen-saturated ethyl acetate for EPR measurement of lipid radicals.

Photofrin/light treatment

K-562 cells were incubated with Photofrin (6–9 μg/ml) for 45 min in PBS solution. After Photofrin-treatment, cells were washed three times with PBS and then resuspended in 500 μl PBS. MCF-7 cells were incubated with Photofrin (6 μg/ml) for 24 h in full medium. After Photofrin-treatment, cells were washed three times with PBS and then resuspended in 500 μl PBS. Cells were then illuminated with visible light (100 J/m^{2}s or 180 J/m^{2}s, 0–20 min) to activate the photosensitizer, thereby initiating the peroxidation process.

RESULTS AND DISCUSSION

Short lifetime of DMPO adducts limits lipid radical analysis

To investigate radical formation during cell membrane lipid peroxidation, K-562 cells were modified with DHA to increase the unsaturation of the cellular membranes. The DHA-enriched K-562 cells were then incubated with Photofrin, a photosensitizer that produces singlet oxygen upon light exposure. Singlet oxygen reacts with the double bonds of unsaturated fatty acids, forming lipid hydroperoxides [28,29]. Ferrous iron initiates radical chain reactions by reacting with these lipid hydroperoxides. As shown in Fig. 1A, K-562 cells incubated with 9 μg/ml Photofrin for 45 min produce a weak DMPO spin adduct signal upon addition of ferrous iron in the dark. This DMPO spin adduct is derived from an oxygen-centered radical and decays in minutes (data not shown). Upon light exposure, lipid-derived oxygen-centered and carbon-centered DMPO spin adducts increase during the first 10 min as shown in Fig. 1B–1C. However, after 20 min of light exposure with 250 μM O_2 initial concentration, most of the oxygen-centered radicals have decayed, Fig. 1D. Because this experiment is done in a closed system, the concentration of oxygen decreases over time. This decrease will result in a higher steady-state concentration of carbon-centered radicals, thereby increasing the rate of destruction of spin adducts, reaction 3 above. Thus, the oxygen-centered spin adducts will have been destroyed and only a low level of carbon-centered radicals are observed.

A similar time-dependent appearance and disappearance of oxygen-centered radicals can be seen in Fe^{2+}-mediated DHA oxidation with 250 μM O_2 initial concentration, Figure 1E–G. These data show that lipid-derived radicals, especially oxygen-centered lipid radicals, are quite unstable and that EPR spin trapping of these radicals has severe limitations. We hypothesize that the interruption of the termination reaction (reaction 3) is key to study the reaction of oxygen-centered lipid radicals successfully. We propose that coupling an extraction process with EPR spin trapping would increase the usefulness of EPR studies of lipid peroxidation.

Extraction stops the lipid peroxidation cycle

In order that lipid radical profiles versus time can be determined, it is important that the unreacted DMPO remains in the aqueous phase during the extraction process. This will prevent continued formation of spin adducts from background lipid oxidation. To verify that DMPO locates principally in the aqueous phase we subjected an aqueous solution of DMPO (Fig. 2) to our extraction protocol and determined the phase distribution of DMPO after extraction using UV measurements [30]. The aqueous phase after the extraction was purged with nitrogen to remove ethyl acetate residue, Fig. 2B–2E. The spectrum of DMPO in the aqueous phase after ethyl acetate extraction and removal of virtually all ethyl acetate with 30 min N_2-purging (Fig. 2E) was nearly identical with the initial 100 μM aqueous solution of DMPO (Fig. 2F). These data show that DMPO locates principally in the aqueous phase after ethyl acetate extraction under our experimental conditions. This limits the interference of background signals due to the extraction process and allows the probing of time-profiles of radical formation during lipid peroxidation. Similar results were observed in aqueous solutions of DMPO subjected to Folch extraction ($CHCl_3$/MeOH, data not shown). Thus, extraction appears to be a good method to separate the reactants of lipid peroxidation, thereby stopping the reaction, Scheme 2. Stopping the reaction will increase the lifetime of the spin adducts formed, permitting their detection.

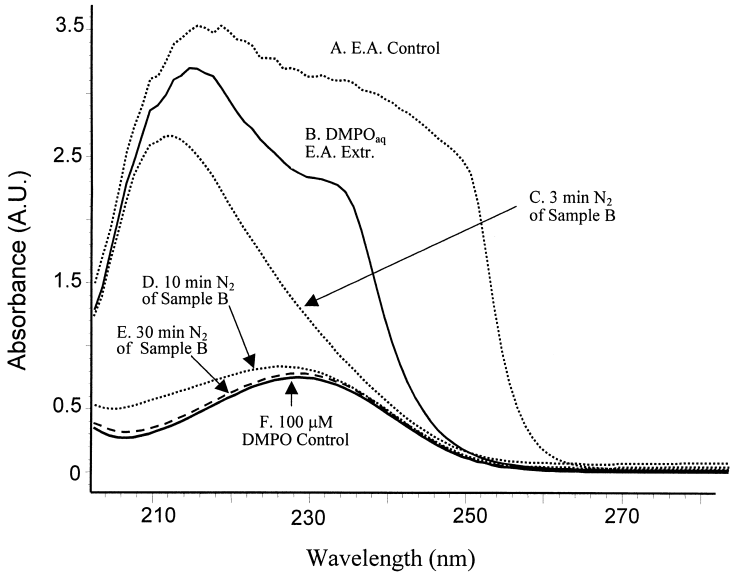

Fig. 2. UV spectra of DMPO in aqueous solution pre- and postethyl acetate extraction ($\varepsilon_{225\ nm} \approx 7800\ M^{-1}{\cdot}cm^{-1}$ [30]). (E.A. is ethyl acetate). (A) Ethyl acetate 100%, please note that absorbance readings ≥ 2 are above the limits for reliability for the instrument; (B) Spectrum of a 100 μM aqueous solution of DMPO that has been subjected to ethyl acetate extraction (H_2O/ethyl acetate = 1/2 (v/v)); (C) Spectrum B after purging with N_2 gas for 3 min, the change in the spectrum demonstrates that the ethyl acetate that partitioned into the buffer is being purged by the N_2; (D) Spectrum B after purging with N_2 gas for 10 min; (E) Spectrum B after purging with N_2 gas for 30 min. The absorbance at 225 nm is about 0.77, virtually all the ethyl acetate has been removed at this time; (F) 100 μM aqueous solution of DMPO. The absorbance at 225 nm is about 0.76.

Extraction increases stability of DMPO spin adducts formed from DHA oxidations

To test our hypothesis that extraction will stabilize the lipid-derived DMPO spin adducts we applied ethyl acetate extraction to a lipid peroxidation experiment using DHA as the unsaturated lipid. As seen in Fig. 3A, the EPR spectrum shows only two major radical species at 5 min after addition of ferrous iron. The spectrum constantly changes (refer to Fig. 1) resulting in only 2–3 min being available to collect the real-time EPR signal. However, combining EPR with ethyl acetate extraction, DMPO spin adducts can be detected in both aqueous and ethyl acetate phases; with this approach we are able to observe at least five different radical species. Two different long-chain DMPO adducts are observed in the ethyl acetate phase, Fig. 3B, while at least three radical species are detected in the aqueous phase, Fig. 3C. In contrast to the very short lifetime (<20 min, Fig. 1) without extraction, the radical adducts in both phases are much more stable after extraction (>10 h). Different types of radical adducts will be detected in different phases using our experimental protocol (Scheme 2). In our protocol for the detection of the radical adducts in the organic phase, the ethyl acetate-phase is evaporated to dryness using nitrogen or argon. Then the spin adducts are resuspended in 100% ethyl acetate. Because DMPO is a highly volatile compound, it will be removed from the ethyl acetate-phase with nitrogen-purging. Likewise, because DMPO/$^{\bullet}$OH ($a^N \approx$ 13.7 G, $a^H \approx$ 10.4 G in ethyl acetate phase) is a quite small molecule, it too will evaporate upon purging with nitrogen (EPR data not shown). Also, other species such as DMPO/$^{\bullet}$OOH ($a^N \approx$ 13.0 G, $a^H \approx$ 10.5, and 1.4 G in ethyl acetate phase) and the DMPO adducts of DMSO-derived radicals ($CH_3O^{\bullet}$ and $^{\bullet}CH_3$), will also evaporate during N_2-purging. Therefore, the species ($a^N \approx$ 13.5 G, $a^H \approx$ 10.2 G; $a^N \approx$ 12.8 G, $a^H \approx$ 6.85, 1.9 G) in the ethyl acetate phase are most likely long-chain lipid adducts of DMPO. The separation of the mediator of oxidation (iron, aqueous phase) from the substrate (unsaturated lipid, organic phase) by extraction not only stabilizes the spin adducts, but also allows the detection of different types of radicals in different phases.

Assignment of DMPO adducts observed after extraction

Due to the longer lifetime of DMPO adducts post-extraction, it was possible to do signal averaging over a longer time to generate spectra of good enough quality so that assignment of radical species is possible. Using the extraction protocol, lipid-chain radicals were detected in the ethyl acetate phase, while smaller radicals ($R^{\bullet}$, $HO^{\bullet}$, $RO^{\bullet}$) were mostly present in the aqueous phase. For example, when we applied ethyl acetate extraction at 5 min after addition of Fe^{2+} to the DHA oxidation experiment, we were able to use simulation approaches to

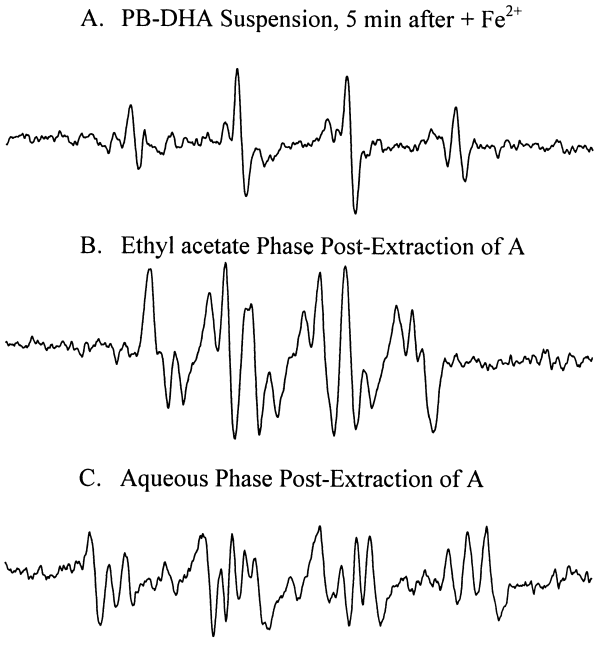

Fig. 3. Extraction with ethyl acetate increases the lifetime of DMPO adducts observed during DHA lipid peroxidation. The reaction system contained 5 mM DHA incubated with 50 mM DMPO, 55 μM DTPA, 250 μM O_2, and 50 μM Fe^{2+}. (A) EPR scans were initiated 5 min after addition of Fe^{2+}. The spectrum is constantly changing; refer to Fig. 1(E–G). Thus, only a 2–3 min window is available to collect specific spectra; this short time limits the opportunity to signal average data to enhance very weak EPR signals. This spectrum is the result of 12 signal-averaged scans collected over a total of 2 min; (B) The lifetimes of spin adducts in the ethyl acetate phase post-extraction are much longer (>10 h), allowing signal averaging techniques to be used to great advantage. This spectrum is the result of 120 signal-averaged scans collected over a total of 20 min of the ethyl acetate phase; (C) The lifetimes of spin adducts in the aqueous phase post-extraction are also much longer (>10 h). This spectrum is the result of 120 signal-averaged scans collected over a total of 20 min of the aqueous phase.

assign the three major radical adducts observed in the aqueous phase post-extraction, Fig. 4. The radical adduct with hyperfine splitting constants: $a^N \approx a^H \approx 14.8$ G could be either DMPO/RO$^\bullet$ or DMPO/HO$^\bullet$. The spin adducts DMPO/HO$^\bullet$ and DMPO/RO$^\bullet$ can have very similar hyperfine splittings when RO$^\bullet$ is a *tert*-alkoxyl radical [31,32]. The DMPO/HO$^\bullet$ ($a^N \approx a^H \approx 14.8$ G) species can arise from a nonradical pathway [33] or from the hydrogen peroxide-mediated Fenton reaction [12,34]. Recent work suggests that alkoxyl radicals usually have quite different hyperfine splittings than DMPO/HO$^\bullet$ [35]; thus, DMPO/HO$^\bullet$ is the best assignment. The other two adducts are short-chain carbon-centered radicals ($a^N{}_1 \approx$ 15.2 G, $a^H{}_1 \approx 18.9$ G; $a^N{}_2 \approx 15.8$ G, $a^H{}_2 \approx 22.6$ G) formed by fragmentation of lipid chains undergoing β-scission [36–38]. In the organic phase post-extraction, using simulation, we have tentatively assigned the radical adducts as two long-chain lipid radicals, i.e., an as-yet-unknown lipid radical adduct of DMPO ($a^N \approx$ 13.5 G, $a^H \approx 10.2$ G) and a lipid alkoxyl adduct DMPO/LO$^\bullet$ ($a^N \approx 12.8$ G; $a^H \approx 6.85$ G, 1.9 G), Fig. 5. Lipid peroxyl radical adducts seem to have lifetimes much too short for them to be observed in room temperature solutions [31,32,39]. The exact nature of the alkoxyl radical is not yet known. The species LO$^\bullet$ is expected to have a very short lifetime, as cyclization and β-scission are

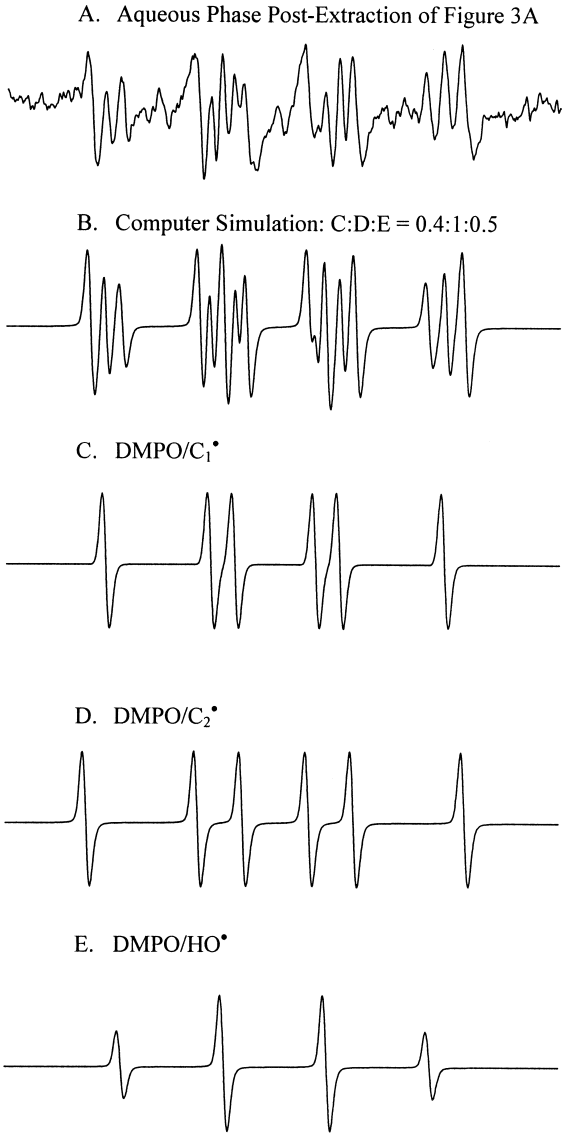

Fig. 4. At least three DMPO adducts are clearly observed in the aqueous phase post-extraction in the DHA-peroxidizing system of Fig. 3. (A) EPR spectrum in the aqueous phase of DHA oxidation system, e.g., Fig. 3C; (B) Composite simulation using a ratio of 0.4:1:0.5 for the two carbon-centered radical spin adducts (DMPO/$C_1^\bullet$, DMPO/$C_2^\bullet$), and DMPO/HO$^\bullet$; C, D, and E respectively; (C) Simulated spectrum of DMPO/$^\bullet C_1$: $a^N{}_1 \approx 15.2$ G, $a^H{}_1 \approx 18.9$ G, line width ≈ 0.8 G, Lorentzina/Gaussian ≈ 1.0; (D) Simulated spectrum DMPO/$^\bullet C_2$: $a^N{}_2 \approx$ 15.8 G, $a^H{}_2 \approx 22.6$ G, line width ≈ 1.0 G, Lorentzina/Gaussian ≈ 0.7; (E) Simulated spectrum of HO$^\bullet$: $a^N \approx a^H \approx 14.8$ G, line width ≈ 1.0 G, Lorentzina/Gaussian ≈ 0.7.

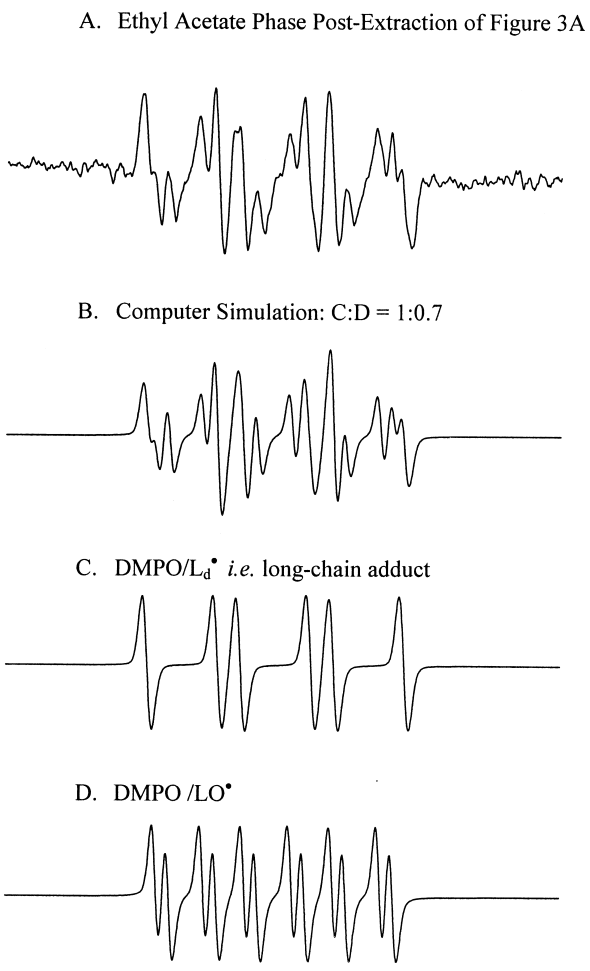

Fig. 5. Two DMPO adducts are observable in the organic phase (ethyl acetate) after extraction of the DHA-peroxidizing system of Fig. 3. (A) EPR spectrum in the ethyl acetate phase of DHA oxidation system, e.g., Fig. 3B; (B) Composite simulation using a ratio of 1:0.7 for a long-chain radical adduct and an alkoxyl radical adduct DMPO/LO$^\bullet$, C, and D respectively; (C) Simulated spectrum of DMPO/L$_d^\bullet$: $a^N \approx 13.5$ G, $a^H \approx 10.2$ G, line width ≈ 1.3 G, Lorentzina/Gaussian ≈ 0.7; (D) Simulated spectrum of DMPO/LO$^\bullet$: $a^N \approx 12.8$ G, $a^H \approx 6.85$ G; 1.9 G, line width ≈ 1.1 G, Lorentzina/Gaussian ≈ 0.5. A small amount of the low molecular weight spin adducts, such as DMPO/HO$^\bullet$ and DMPO/HOO$^\bullet$ can partition in ethyl acetate phase upon extraction with $a^N \approx 13.7$ G, $a^H \approx 10.4$ G; $a^N \approx 13.0$ G, $a^H \approx 10.5$, and 1.4 G, respectively. However, these adducts can be removed from the ethyl acetate phase by complete evaporation using N_2-purging. Thus, spectrum C and D should be assigned to be long-chain radical adducts.

facile processes [40]. The lifetimes of all adducts (post-extraction) observed are significantly increased (often persisting for hours), thus signal-averaging techniques can be employed and the profile of radical formation can be determined.

Detection of lipid radical adducts from K-562 cells

Using our extraction protocol, we have for the first time detected the formation of long-chain, oxygen-centered, lipid radicals from cells. We exposed K-562 cells to singlet oxygen to seed lipid hydroperoxides into the cell membranes. Then, after addition of

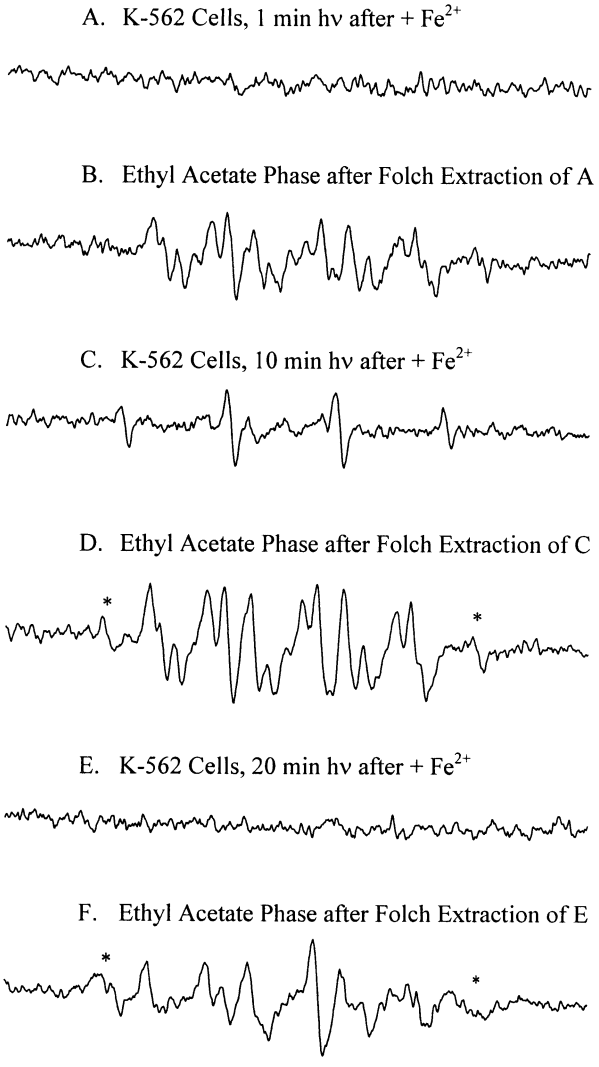

Fig. 6. Lipid radicals can be trapped by DMPO from intact K-562 cells using the combination of EPR and Folch extraction. DHA-modified K-562 cells (5×10^6 cells/ml) were incubated with 6 μg/ml Photofrin followed by a 10 min exposure to visible light (100 W/m^2). This introduces LOOH into cell membrane via a nonradical mechanism. With 250 μM initial [O_2], 150 mM DMPO, 110 μM DTPA, and 100 μM Fe^{2+} were introduced to initiate free radical lipid peroxidation. (A) This spectrum is from the K-562 cell suspension described above, but cell sample received an additional 1 min light expose after introduction of Fe^{2+}; (B) EPR spectrum from the organic phase in ethyl acetate after Folch extraction of sample A; (C) Sample A, but with 10 min light expose after introduction of Fe^{2+}; (D) EPR spectrum from the organic phase in ethyl acetate after Folch extraction of sample C. The principal species are assigned as two long-chain adducts: DMPO/LO$^\bullet$ ($a^N \approx 12.9$ G, $a^H \approx 6.95$ G, 1.9 G); DMPO/L$_d^\bullet$ ($a^N \approx 13.6$ G, $a^H \approx 10.4$ G); and DMPO/OL$^\bullet$ or DMPO/L$^\bullet$ ($a^N \approx 13.8$ G, $a^H \approx 22.7$ G), the two outermost lines are marked by *; (E) Sample A, but with 20 min light expose after introduction of Fe^{2+}; (F) EPR spectrum from organic phase in ethyl acetate after Folch extraction of sample E. A, C, and E are spectra from 12 signal-averaged scans collected over a total of 2 min; B, D, and F are spectra from 180 signal-averaged scans collected over a total of 30 min.

DMPO and DTPA to the cell suspension, free radical processes were initiated by addition of ferrous iron. Chelators such as EDTA and DTPA can enhance free radical formation from Fe^{2+}-initiated oxidations [8,41]. EPR-detectable species were observed from K-562 cells in both the cell suspension without extraction (Fig. 6A, C, and E) and the organic phase after Folch extraction (Fig. 6B, D, and F).

In the cell suspension undergoing oxidative stress, only an EPR signal having a 1:2:2:1 intensity pattern (DMPO/$HO^{\bullet}$) was clearly observed, Fig. 6C. Using our extraction protocol, we were able to remove DMPO/$HO^{\bullet}$ from the organic phase; however, there were at least two EPR detectable species ($a_1^N \approx 13.6$ G, $a_1^H \approx 10.4$ G; and $a_2^N \approx 12.9$ G, $a_2^H \approx 6.95$ G, 1.9 G) remaining in the ethyl acetate phase, Fig. 6B, D, and F. The species in the ethyl acetate phase are consistent with being long-chain lipid radical adducts similar to those observed in experiments with DHA presented above. A 1:2:2:1 EPR signal ($a^N \approx a^H \approx 14.8$ G) can also be observed in Photofrin control experiments (no cells) upon light exposure. However, this species was not observed in the ethyl acetate phase after extraction (data not shown). In the spectra shown in Fig. 6D and F, we also observed a carbon-centered radical adduct (two outmost lines marked by *). We propose that this adduct ($a^N \approx 13.8$ G, $a^H \approx 22.7$ G) is a lipid alkyl ($L^{\bullet}$) or perhaps epoxyallylic ($OL^{\bullet}$) radical. Because it arises later in the experiment it will be at a time when there has been a significant decrease in oxygen concentration, thus the probability of detecting carbon-centered radicals is increased. This success in the detection of different lipid radicals in cell systems should open new doors to radical studies using cells and tissues.

We have also had success in applying this extraction protocol to the study of lipid peroxidation in adherent cells, such as MDCK cells [42] and MCF-7 cells [43]. The long-chain lipid radical adducts observed in the ethyl acetate phase of experiments, using adherent cells, were parallel to our K-562 results.

Detection of lipid radical adducts from LDL oxidation

The oxidation of LDL is thought to be an important mechanistic component of atherosclerosis [44]. We have applied our extraction approach to the detection of lipid-derived radicals during copper-mediated LDL oxidation. A suspension of LDL in PB was treated with DMPO and Cu^{2+}, and then examined by EPR with or without Folch extraction. Similar to the results observed with K-562 cells, LDL produces EPR detectable spin adducts in both the PB-LDL suspension and the organic phase, Fig. 7. The EPR signal in the PB-LDL suspension having a 1:2:2:1 intensity pattern was only observed for the first 10 min after Cu^{2+} was introduced. The two radical

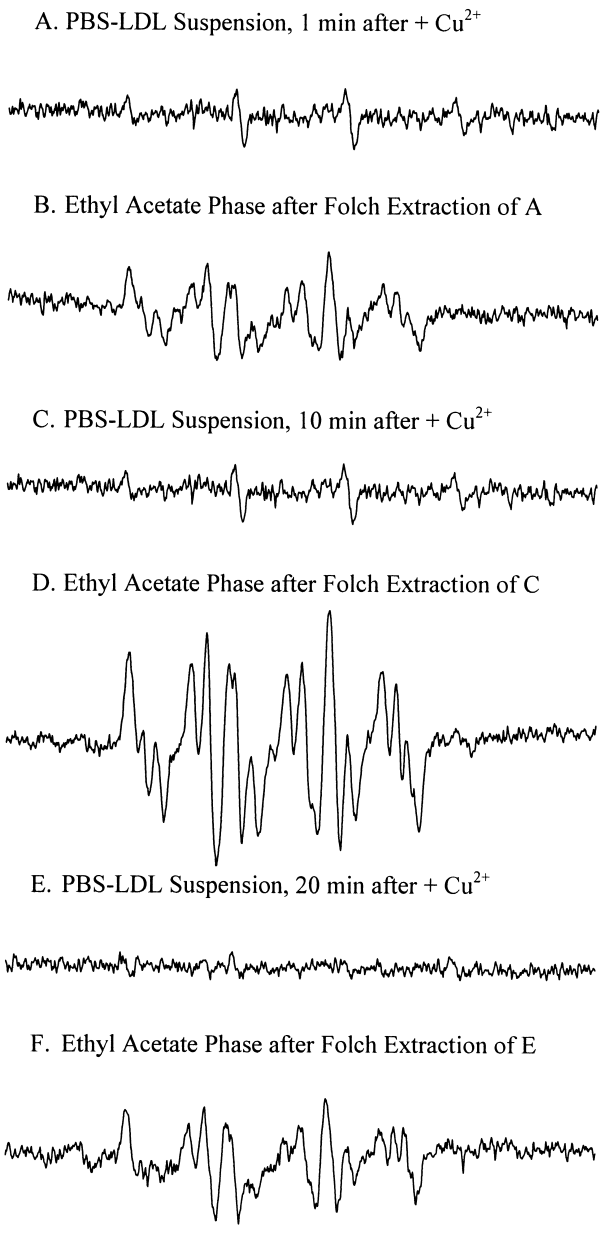

Fig. 7. Lipid radical production from LDL oxidation. A typical incubation for an EPR experiment consisted of 2.2 mg/ml of LDL, 100 mM DMPO, and 100 μM Cu^{2+} in PB. To analyze spin adducts in PB-LDL suspension, the incubation mixture (500 μL) with 250 μM initial [O_2], was transferred into an EPR flat cell for EPR measurement. For analysis of spin adducts in organic extracts, the incubation mixture (500 μL) was extracted using the Folch method before EPR measurement. (A) EPR spectrum of the PB-LDL suspension oxidized 1 min after introduction of Cu^{2+}; (B) EPR spectrum of the organic phase of sample A post-extraction; (C) Sample A; but run EPR 10 min after introduction of Cu^{2+}; (D) EPR spectrum of the organic phase of sample C post-extraction long-chain radicals (DMPO/$LO^{\bullet}$: $a^N \approx 12.9$ G, $a^H \approx 6.95$ G, 1.9 G; DMPO/$L_d^{\bullet}$: $a^N \approx 13.6$ G, $a^H \approx 10.4$ G); (E) Sample A; but run EPR 20 min after introduction of Cu^{2+}; (F) EPR spectrum of the organic phase of sample E post-extraction. A, C, and E are spectra from 3 signal-averaged scans collected over a total of 2 min; B, D, and F are spectra from 60 signal-averaged scans collected over a total of 40 min.

adducts observed in the ethyl acetate phase are assigned as long-chain lipid adduct of DMPO ($a^N \approx 13.6$ G, $a^H \approx 10.4$ G) and DMPO/LO$^\bullet$ ($a^N \approx 12.9$ G, $a^H \approx 6.95$ G, 1.9 G). Thus, the extraction approach is also of value in studying LDL oxidation.

Determining the time profile of radical detection

In Figs. 6 and 7 limited information is available on radical production from K-562 cells and LDL experiments without extraction. A great deal more information becomes available upon extraction. Not only are more radicals observed, but time profiles for radical production/decay can be obtained by initiating the extraction at different time points in the peroxidation process. See B, D, and F in Figs. 6 and 7. Any given spectrum in a spin trapping experiment represents the balance between spin adduct formation and spin adduct decay. Thus, if spin trap could be introduced at different time points additional information could be gathered on reaction profiles vs. time.

Radical adducts detected by EPR-extraction are LOOH-derived

We have had very limited success in our laboratory detecting free radicals from adherent cells [45]. However, we have found that our extraction approach can be a great aid. To demonstrate this, we have used MCF-7 cell lines that have been transfected with PhGPx to increase the activity of this enzyme [41]. PhGPx removes phospholipid hydroperoxides from cell membranes [46, 47]:

$$2\ \mathrm{GSH} + \mathrm{Ph\text{-}LOOH} \xrightarrow{\mathrm{PhGPx}} \mathrm{Ph\text{-}LOH} + \mathrm{GSSG} + \mathrm{H_2O} \quad (4)$$

Cells were treated with Photofrin and light to produce lipid hydroperoxides, Ph-LOOH. If ferrous iron is added immediately upon cessation of illumination, as expected [48] all cell lines (wild type MCF-7, Neo-transfectants, and the MCF-7-transfected cell lines with high Ph-GPx activity) produced the same amount of lipid-derived radicals (not shown). But if the cells were allowed to recover for 6 h in the dark (37°C in full media) before introduction of ferrous iron, the cells with high PhGPx activity showed essentially no radical production while Wt and Neo cells had considerable radical production, Fig. 8.

These experiments show that our extraction technique can be used for adherent cells. This is the first demonstration that lipid-derived oxygen-centered radical formation could be observed from adherent cells. These data provide evidence that the radicals detected by this EPR-extraction method are derived from membrane lipid oxidation.

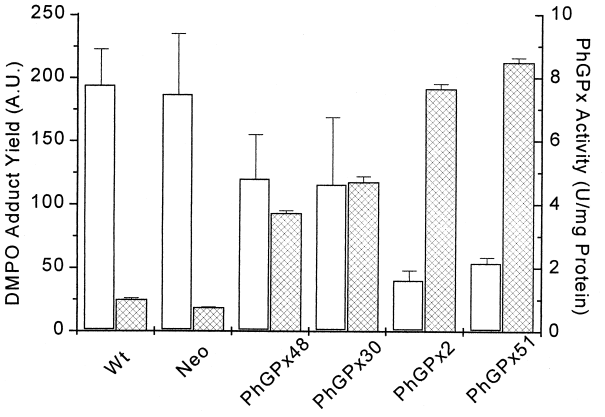

Fig. 8. Radical yield from MCF-7 cells and their PhGPx transfectants. The open bar represents DMPO adduct yield; and the checked bar represents PhGPx activity. A yield of 70 A.U. was considered to be background noise-level. Cells were pretreated with 6 μg/ml Photofrin for 24 h, and exposed to light (5 J/m^{2}s) for 5 min. Cells were then incubated in full media for 6 h. After that, cells were washed and incubated with 100 mM DMPO and 100 μM ferrous iron for 5 min in PBS at room temperature. The lipids and lipid radical spin adducts were extracted with chloroform:methanol (2:1, *v/v*). The chloroform layer was dried under argon, and redissolved in 500 μl degassed ethyl acetate. The ethyl acetate was immediately transferred to an EPR flat cell and EPR scans started. The long-chain radicals ($a^N \approx 15.2$ G, $a^H \approx 10.2$ G) are quantitated and used to represent potential radical formation from cell oxidations. Data are representative of three experiments. Error bar represents standard derivation.

CONCLUSIONS

We conclude that EPR spin trapping coupled with organic extraction can stabilize lipid-derived spin adducts, thus overcoming some of the disadvantages of EPR detection of lipid-derived radicals in biological systems. This will open new doors for the study of the free radical events of biological lipid peroxidation. This method can be easily adapted to study radical production of the lipid-containing components of biological materials, such as suspension cells, adhesive cells, or perhaps tissue. The longer lifetime of spin adducts post-extraction provides an opportunity for identifying the structure of the radicals via EPR, HPLC, and MS. Furthermore, by applying extraction at specific time points, the profile of all lipid-derived radicals can be correlated to the cellular cytotoxicity. This will be a big step forward in our understanding of the free radical mechanism of cellular lipid peroxidation.

Acknowledgements — This work was supported by NIH Grants CA66081 and CA81090.

REFERENCES

[1] Marnett, L. J.; Wilcox, A. L. The chemistry of lipid alkoxyl radicals and their role in metal-amplified lipid peroxidation. In: Rice-Evans, C.; Halliwell, B.; Lunt, G. G., eds. *Free radicals and oxidative stress: environment, drugs and food additives* (Biochemical Society Symposium, Vol. 61). London: Portland Press; 1995:65–72.

[2] Wilcox, A. L.; Marnett, L. J. Polyunsaturated fatty acid alkoxyl radicals exist as carbon-centered epoxyallylic radicals: a key step in hydroperoxide-amplified lipid peroxidation. *Chem. Res. Toxicol.* **6:**413–416; 1993.

[3] Girotti, A. W. Mechanisms of lipid peroxidation. *Free Radic. Biol. Med.* **1:**87–95; 1985.

[4] Gardner, H. W. Oxygen radical chemistry of polyunsaturated fatty acids. *Free Radic. Biol. Med.* **7:**65–86; 1989.

[5] Wagner, B. A.; Buettner, G. R.; Burns, C. P. Free radical-mediated lipid peroxidation in cells: oxidizability is a function of cell lipid bis-allylic hydrogen content. *Biochemistry* **33:**4449–4453; 1994.

[6] Wagner, B. A.; Buettner, G. R.; Burns, C. P. Increased generation of lipid-derived and ascorbate free radicals by L1210 cells exposed to the ether lipid edelfosine. *Cancer Res.* **53:**711–713; 1993.

[7] Buettner, G. R.; Kelley, E. E.; Burns, C. P. Membrane lipid free radicals produced from L1210 murine leukemia cells by Photofrin photosensitization: An EPR spin trapping study. *Cancer Res.* **53:**3670–3673; 1993.

[8] Qian, S. Y.; Buettner, G. R. Iron and dioxygen chemistry is an important route to initiation of biological free radical oxidations: an electron paramagnetic resonance spin trapping study. *Free Radic. Biol. Med.* **26:**1447–1456; 1999.

[9] Kelley, E. E.; Buettner, G. R.; Burns, C. P. Production of lipid-derived free radicals in L1210 murine leukemia cells is an early event in the photodynamic action of Photofrin. *Photochem. Photobiol.* **64:**576–580; 1997.

[10] Wagner, B. A.; Buettner, G. R.; Oberley, L. W.; Burns, C. P. Sensitivity of K-562 and HL60 cells to edelfosin, an ether lipid drug, correlates with production of active oxygen species. *Cancer Res.* **58:**2809–2816; 1998.

[11] Schafer, F.; Buettner, G. R. Acidic pH amplifies iron-mediated lipid peroxidation in cells. *Free Radic. Biol. Med.* **28:**1175–1181; 2000.

[12] Chamulitrat, W.; Hughes, M. F.; Eling, T. E.; Mason, R. P. Superoxide and peroxyl radical generation from the reduction of polyunsaturated fatty acid hydroperoxides by soybean lipoxygenase. *Arch. Biochem. Biophys.* **290:**153–159; 1991.

[13] Davies, M. J. Detection of peroxyl and alkoxyl radicals produced by reaction of hydroperoxides with heme-proteins by electron spin resonance spectroscopy. *Biochim. Biophys. Acta* **964:**28–35; 1988.

[14] Davies, M. J.; Slater, T. F. Studies on the metal-ion and lipoxygenase-catalysed breakdown of hydroperoxides using electron-spin-resonance spectroscopy. *Biochem. J.* **245:**167–173; 1987.

[15] Schaich, K. M.; Borg, D. C. Solvent effects in the spin trapping of lipid oxyl radicals. *Free Radic. Res. Comm.* **9:**267–278; 1990.

[16] Kocherginsky, N.; Swartz, H. M. Chemical reactivity of nitroxides. In: Kocherginsky, N.; Swartz, H. M., eds. *Nitroxide spin labels: reactions in biology and chemistry*. Boca Raton, FL: CRC Press; 1995:48–49.

[17] McCay, P. B.; Lai, E. K.; Poyer, J. L.; DuBose, C. M.; Janzen, E. G. Oxygen- and carbon-centered free radical formation during CCl4 metabolism: observation of lipid radicals in vivo and in vitro. *J. Biol. Chem.* **259:**2135–2143; 1984.

[18] Janzen, E. G.; Towner, R. A.; Haire, D. L. Detection of free radicals generated from the in-vitro metabolism of carbon tetrachloride using improved ESR spin trapping techniques. *Free Radic. Res. Commun.* **3:**357–364; 1987.

[19] Albano, E.; Lott, K. A.; Slater, T. F.; Stier, A.; Symons, M. C.; Tomasi, A. Spin-trapping studies on the free-radical products formed by metabolic activation of carbon tetrachloride in rat liver microsomal fractions isolated hepatocytes and in vivo in the rat. *Biochem. J.* **204:**593–603; 1982.

[20] Buettner, G. R. In the absence of catalytic metals ascorbate does not autoxidize at pH 7: ascorbate as a test for catalytic metals. *J. Biochem. Biophys. Methods* **16:**27–40; 1988.

[21] Kotake, Y.; Reinke, L. A.; Tanigawa, T.; Koshida, H. Determination of the rate of superoxide generation from biological systems by spin trapping: use of rapid oxygen depletion to measure the decay rate of spin adducts. *Free Radic. Biol. Med.* **17:**215–223; 1994.

[22] Hatch, F. T.; Lees, R. S. Practical methods for plasma lipoprotein analysis. *Adv. Lipid Res.* **6:**2–68; 1968.

[23] Guffy, M. M.; North, J. A.; Burns, C. P. Effect of cellular fatty acid alteration on Adriamycin sensitivity in cultured L1210 leukemia cells. *Cancer Res.* **44:**1863–1866; 1984.

[24] Burns, C. P.; Wagner, B. A. Heightened susceptibility of fish oil polyunsaturate-enriched neoplastic cells to ethane generation during lipid peroxidation. *J. Lipid Res.* **32:**79–87; 1991.

[25] Burns, C. P.; Haugstad, B. N.; Mossman, C. J.; North, J. A.; Ingraham, L. M. Membrane lipid alteration: effect on cellular uptake of mitoxantrone. *Lipids* **23:**393–397; 1988.

[26] Li, A. S. W.; Cummings, K. B.; Roethling, H. P.; Buettner, G. R.; Chignell, C. F. A spin trapping database implemented on the IBM PC/AT. *J. Magn. Reson.* **79:**140–142; 1988.

[27] Buettner, G. R. Spin trapping: ESR parameters of spin adducts. *Free Radic. Biol. Med.* **3:**259–303; 1987.

[28] Jori, G. The molecular biology of photodynamic action. In: Pratesi, R.; Succhi, C. A., eds. *Lasers in photomedicine and photobiology*. Berlin, Germany: Springer-Verlag; 1980:58–66.

[29] Thomas, J. P.; Girotti A. W. Reactivity of photochemically-generated lipid hydroperoxides in cell membranes with glutathione peroxidase. *Photochem. Photobiol.* **49:**153–156; 1989.

[30] Buettner, G. R. On the reaction of superoxide with DMPO/˙OOH. *Free Radic. Res. Comm.* **10:**11–15; 1990.

[31] Krainev, A. G.; Bigelow, D. J. Comparison of 2,2′-azobis (2-amidinopropane) hydrochloride (AAPH) and 2,2′-azobic (2, 4-dimethylvaleronitrile) (AMVN) as free radical initiators: a spin-trapping study. *J. Chem. Soc. Perkin Trans. 2.* 747–754; 1996.

[32] Krainev, A. G.; Williams, T. D.; Bigelow, D. J. Oxygen-centered spin adducts of 5,5-dimethyl-1-pyrroline N-oxide (DMPO) and 2H-imidazole 1-oxides. *J. Magn. Reson. B.* **111:** 272–280; 1996.

[33] Hanna, P. M.; Chamulitrat, W.; Mason, R. P. When are metal ion-dependent hydroxyl and alkoxyl radical adducts of 5,5-dimethyl-1-pyrroline *N*-oxide artifacts? *Arch. Biochem. Biophys.* **296:**640–644; 1992.

[34] Chamulitrat, W.; Iwahashi, H.; Kelman, D. J.; Mason, R. P. Evidence against the 1:2:2:1 quartet DMPO spectrum as the radical adduct of the lipid alkoxyl radical. *Arch. Biochem. Biophys.* **296:**645–649; 1992.

[35] Dikalov, S. I.; Mason, R. P. Reassignment of organic peroxyl radical adducts. *Free Radic. Biol. Med.* **27:**864–872; 1999.

[36] Iwahashi, H.; Parker, C. E.; Tomer, K. B.; Mason, R. P. Detection of the ethyl- and pentyl-radical adducts of alpha-(4-pyridyl-1-oxide)-N-*tert*-butylnitrone in rat-liver microsomes treated with ADP, NADPH and ferric chloride. *Free Radic. Res. Commun.* **16:**295–301; 1992.

[37] North, J. A.; Spector, A. A.; Buettner, G. R. Detection of lipid radicals by electron paramagnetic resonance spin trapping using intact cells enriched with polyunsaturated fatty acid. *J. Biol. Chem.* **267:**5743–5746; 1992.

[38] Iwahashi, H.; Deterding, L. J.; Parker, C. E.; Mason, R. P. Tomer, K. B. Identification of radical adducts formed in the reactions of unsaturated fatty acids with soybean lipoxygenase using continuous flow fast atom bombardment with tandem mass spectrometry. *Free Radic. Res.* **25:**255–274; 1996.

[39] Janzen, E. G.; Krygsman, P. H.; Lindsay, D. A.; Haire, D. L. Detection of alkyl, alkoxyl and alkylperoxyl radicals from the thermolysis of azo-bis-(isobutyronitrile) by ESR spin trapping - evidence for the double spin adducts from liquid-phase chroma-

tography and mass spectroscopy. *J Am. Chem. Soc.* **112:**8279–8284; 1990.
[40] Grossi, L.; Strazzari, S.; Gilbert, B. C.; Whitwood, A. C. Oxiranylcarbinyl radicals from allyloxyl radical cyclization: characterization and kinetic information via ESR spectroscopy. *J. Org. Chem.* **63:**8366–8372; 1998.
[41] Buettner, G. R.; Doherty, T. P.; Patterson, L. K. The kinetics of the reaction of superoxide radical with Fe(III) complexes of EDTA, DETAPAC, and HEDTA. *FEBS Lett.* **158:**143–146; 1983.
[42] Qian, Y.; Buettner, G. R. The EPR detection of lipid-derived radicals during membrane lipid peroxidation of cells. *Free Radic. Biol. Med.* **25**(Suppl.):S106; 1998.
[43] Wang, H.; Buettner, G. R.; Oberley, L. W. Overexpression of human PhGPx in human breast cancer cells (MCF-7): effects on Photofrin photosensitization. *Photochem. Photobiol.* **69**(Suppl.): 36S; 1999.
[44] Steinberg, D.; Parthasarathy, S.; Carew, T. E.; Khoo, J. C.; Witztum, J. L. Beyond cholesterol: modifications of low-density lipoprotein that increase its atherogenicity. *N. Engl. J. Med.* **320:**915–924; 1989.
[45] Flanagan, S. W.; Moseley, P. L.; Buettner, G. R. Increased flux of free radicals in cells subjected to hyperthermia: detection by electron paramagnetic resonance spin trapping. *FEBS Lett.* **431:** 285–286; 1998.
[46] Ursini, F.; Maiorino, M.; Gregolin, C. The selenoenzyme phospholipid hydroperoxide glutathione peroxidase. *Biochim. Biophys. Acta* **839:**62–70; 1985.
[47] Thomas, J. P.; Maiorino, M.; Ursini, F.; Girotti, A. W. Protective action of phospholipid hydroperoxide glutathione peroxidase against membrane-damaging lipid peroxidation. In situ reduction of phospholipid and cholesterol hydroperoxides. *J. Biol. Chem.* **265:**454–461; 1990.
[48] Schafer, F. Q.; Buettner, G. R. Singlet oxygen toxicity is cell-line dependent: a study of lipid peroxidation in nine leukemia cell lines. *Photochem. Photobiol.* **70:**858–867; 1999.

ABBREVIATIONS

DHA—docosahexaenoic acid
DMPO—5,5-dimethyl-pyrroline-1-oxide
DTPA—diethylenetriaminepentaacetic acid
EDTA—ethylenediaminetetratacetic acid
EPR—electron paramagnetic resonance
GSH—glutathione
GSSG—glutathione disulfide
HPLC—high performance liquid chromatography
$L_d^{\bullet}$—lipid-derived radical
LDL—low-density lipoprotein
M.S.—mass spectrometry
PB—potassium phosphate buffer
PBS—potassium phosphate buffer saline (0.9%)
PhGPx—phospholipid hydroperoxide glutathione peroxidase
Ph-LOOH—a phospholipid hydroperoxide in the cell membrane
Ph-LOH—a phospholipid alcohol in the cell membrane
POBN—α-[4-pyridyl-1-oxide]-N-*tert*-butyl nitrone
PUFA—polyunsaturated fatty acid
UV—ultraviolet light